Tertiary Structure Stability of the Hairpin Ribozyme in Its Natural and Minimal Forms: Different Energetic Contributions from a Ribose Zipper Motif†

Dagmar Klostermeier and David P. Millar*

The Scripps Research Institute, Department of Molecular Biology, MB-19, 10550 North Torrey Pines Road, La Jolla, California 92037

Received April 16, 2001; Revised Manuscript Received July 10, 2001

ABSTRACT: The hairpin catalytic motif in tobacco ringspot virus satellite RNA consists of two helix−loop−helix elements on two adjacent arms of a four-way helical junction. The bases essential for catalytic activity are located in the loops that are brought into proximity by a conformational change as a prerequisite for catalysis. The two loops interact via a ribose zipper motif involving the 2′-hydroxyls of A_{10}, G_{11}, A_{24}, and C_{25} [Rupert, P. B., and Ferre d'Amare, A. R. (2001) *Nature 401*, 780−786]. To quantify the energetic importance of the ribose zipper hydrogen bonds, we have incorporated deoxy modifications at these four positions and determined the resulting destabilization of the docked conformer by means of time-resolved fluorescence resonance energy transfer. In a minimal form of the ribozyme, in which the loops are placed on the arms of a two-way helical junction, all modifications lead to a significant loss in tertiary structure stability and altered Mg^{2+} binding. Surprisingly, no significant destabilization was seen with the natural four-way junction ribozyme, suggesting that hydrogen bonding interactions involving the 2′-hydroxyls do not contribute to the stability of the docked conformer. These results suggest that the energetic contributions of ribose zipper hydrogen bonds are highly context dependent and differ significantly for the minimal and natural forms of the ribozyme.

The hairpin ribozyme is a small catalytic RNA motif in the satellite RNA of plant viruses with endonuclease and ligase activities that are required for processing viral replication intermediates (reviewed in ref *1*). In tobacco ringspot virus, the hairpin ribozyme comprises two helix−loop−helix elements that lie on adjacent arms of a four-way helical junction (4WJ).[1] A minimal form of the hairpin ribozyme consists just of the two helix−loop−helix segments. Whereas mutations in the helices are tolerated as long as base pairing is maintained, the nucleotides in the loop regions are essential for activity. As a prerequisite for catalysis, a conformational change of the junction has to occur that brings the two loops into proximity. Early evidence for docking into a compact structure that involves a kink at the helical junction came from activity studies of ribozyme constructs with variable length linkers between the two helix−loop−helix elements (*2*, *3*). Cross-linking studies showed that the docked conformer is the catalytically active species (*4*, *5*). Kinetic measurements of domain docking employing fluorescence resonance energy transfer (FRET) also indicate that docking is required for catalysis (*6*).

A variety of biochemical and biophysical methods have been used to define the global fold of the docked hairpin ribozyme, the interface between the two subdomains, and specific tertiary interactions (for a review see ref *1*). Steady-state FRET experiments have been used to probe the metal ion-induced folding and the global geometry of the hairpin ribozyme in its natural 4WJ form (*7*, *8*). Hydroxyradical footprinting studies of a minimal two-way junction (2WJ) ribozyme revealed the existence of a solvent-protected catalytic core involving nucleotides G_{11}-A_{14}, C_{25}-C_{27}, A_{38}, and U_{42}-A_{43} (*9*).

Recently, a crystal structure of the hairpin ribozyme in the docked conformation was solved (*10*, PDB code 1HP6). This structure provides the first direct view of the docking interface, revealing a network of interactions between loops A and B. One of the prominent features is a ribose zipper formed between the N^3 positions of A_{10} and A_{24}, and the 2′-hydroxyls of A_{10}, G_{11}, A_{24}, and C_{25} (Figure 1A). Different models for a ribose zipper-like interaction had been proposed on the basis of early biochemical studies that identified the 2′-hydroxyls of A_{10}, G_{11}, A_{24}, and C_{25} as crucial for catalytic activity (*4*, *11*), from nucleotide analogue interference mapping (*12*) and from studies using different 2′-modified hairpin ribozymes (*13*). The actual hydrogen bonding network in the crystal structure has been predicted correctly by Earnshaw et al. (*4*).

Classical ribose zippers, in which a 2′-hydroxyl accepts a hydrogen bond from the 2′-hydroxyl of its partner, and in turn donates a hydrogen bond to a base nitrogen or oxygen of the partner (one tooth), have also been found in the *Tetrahymena* ribozyme (*14*), the hepatitis delta virus ribozyme (*15*), and the L11 binding domain of 23S rRNA (*16*, *17*).

While biochemical data indicate that the 2′-hydroxyls that participate in the ribose zipper are functionally important, it is unclear whether they stabilize the docked conformer or

† This work was supported by NIH Grant No. GM 58873 (to D.P.M) and an EMBO fellowship (to D.K.)

* Corresponding author. Phone: (858) 784-9870, fax: (858) 784-9067, e-mail: millar@scripps.edu.

[1] Abbreviations: 2WJ, 3WJ, 4WJ: two-way, three-way, four-way helical junction; FRET: fluorescence resonance energy transfer; trFRET: time-resolved fluorescence resonance energy transfer.

10.1021/bi010773f CCC: $20.00
Published on Web 08/18/2001

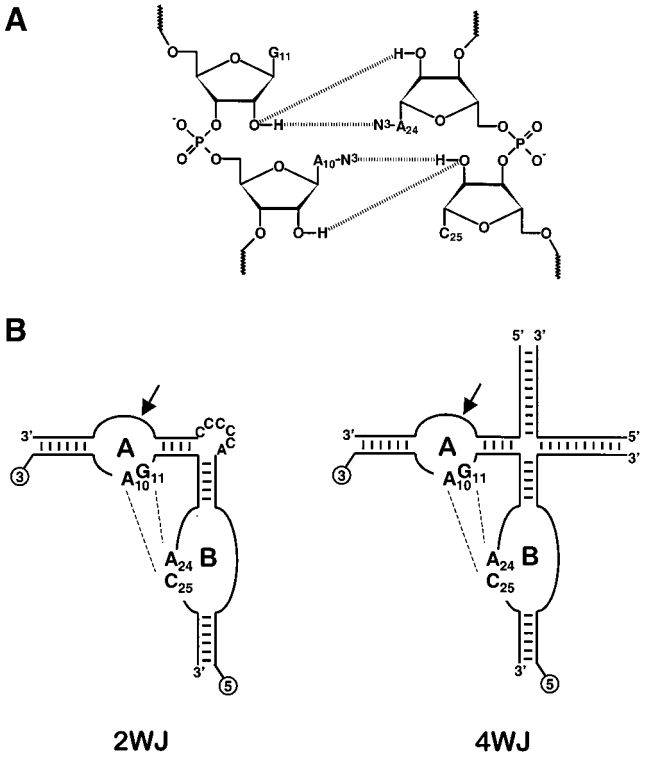

FIGURE 1: Hydrogen bonding pattern in the ribose zipper and hairpin ribozyme constructs studied. (A) Ribose zipper between A_{10} and G_{11} in loop A and A_{24} and C_{25} in loop B. A_{10} donates a hydrogen bond via the 2′-OH to the 2′-O of C_{25}, and the C_{25} 2′-OH donates to N^3 of A_{10}. A_{24} donates a hydrogen bond via its 2′-OH to the 2′-O of G_{11}, which in turn donates to the N^3 of A_{24} (*10*). (B) Minimal (2WJ, left) and natural (4WJ, right) ribozyme−substrate complexes labeled with Cy3 (3) and Cy5 (5). The nucleotides involved in the ribose zipper are indicated in each case. 2′-Deoxy modifications were introduced at each position to determine the influence of each 2′-hydroxyl on ribozyme docking. Tandem deoxy modifications at A_{10} and C_{25}, G_{11} and A_{24}, and A_{10} and G_{11} were also examined. In all cases, a deoxy modification was also introduced at the cleavage site (arrow) to prevent cleavage.

are directly involved in catalysis. In kinetic docking experiments, ribozymes with deoxy modifications at A_{10} and G_{11} show a reduced docking amplitude (*6*), indicating that they form interactions stabilizing the docked ribozyme in the ground state. Similarly, steady-state FRET experiments revealed that deoxy modifications at A_{10} and C_{25} reduce docking to some extent (*18*). The thermodynamic basis for tertiary structure formation in the hairpin ribozyme has recently been examined by a trFRET analysis of ribozyme−substrate complexes doubly labeled with donor and acceptor fluorophores (*19*, *20*). The analysis determines the equilibrium distribution of docked and extended conformers, which defines the free energy of docking, ΔG_{dock}. Comparison of constructs where the two loops were placed on two adjacent arms in a two-way, three-way, and four-way helical junction (2WJ, 3WJ, 4WJ) revealed that the 4WJ promotes docking (*19*). A subsequent thermodynamic analysis based on UV melting profiles and trFRET experiments revealed that the 4WJ favors docking due to a lower entropic penalty for docking as compared to the 2WJ and 3WJ ribozymes (*20*), supporting the notion that the 4WJ of the natural hairpin ribozyme provides a rigid structural framework for catalytic activity.

The comparative study of docking energetics in the different ribozyme junctions also revealed a significantly larger docking enthalpy in the 2WJ as compared with the 4WJ (*20*). Assuming that the docking interface is similar in both forms of the ribozyme, this result suggests that the energetic contribution of a given tertiary contact may vary depending on the overall geometry of the ribozyme−substrate complex. To investigate this possibility, we used trFRET to examine the influence of 2′-deoxy modifications at positions A_{10}, G_{11}, A_{24}, and C_{25} on the stability of the docked ribozyme in both the minimal (2WJ) and the natural (4WJ) hairpin ribozymes (Figure 1B). The results allow us to compare the energetic contributions of the ribose zipper hydrogen bonds to the stability of the docked ribozyme−substrate complex in the context of both the minimal and natural forms of the ribozyme.

EXPERIMENTAL PROCEDURES

Preparation of RNA Samples. RNA strands were purchased from Dharmacon, Boulder, CO. The sequences were 5′-Cy3-AAA UAG AGA AGC GAA CCA GAG AAA CAC ACG CC-3′ and 5′-(Cy5-)GGC GUG GUA CAU UAC CUG GUA CCC CCU CGC dAGU CCU AUU U-3′ (2WJ), or 5′-(Cy5-)-GGC GUG GUA CAU UAC CUG GUA CGA GUU GAC-3′, 5′-GUC AAC UCG UGG UGG CUU GC-3′, 5′-GCA AGC CAC CUC GCdA GUC CUA UUU-3′ (4WJ). The modifications introduced were dA_{10}, dG_{11}, dA_{24}, dC_{25}, $dA_{10}G_{11}$, $dA_{10}C_{25}$, and $dG_{11}A_{24}$, all in the 5′-Cy3-labeled strand. A dA_9 modification was used as a control for nonspecific effects. The RNA was purified via denaturing gel electrophoresis and reverse phase HPLC using an eluent system of acetonitrile and aqueous triethylammonium acetate. RNA complexes were prepared in 50 mM Tris/HCl, pH 7.5, 12 mM $MgCl_2$ at a concentration of 1 μM donor strand and 2 μM of all other strands and were annealed by heating to 70 °C for 2 min and cooling to ambient temperature within 5 min. For Mg^{2+} titrations and kinetic measurements, the ribozyme was annealed in 50 mM Tris/HCl, pH 7.5, 100 mM NaCl (2WJ) or in 50 mM Tris/HCl, pH 7.5, 10 μM $MgCl_2$ (4WJ).

Fluorescence Measurements. Ion titrations and kinetic experiments were performed in an SLM Aminco SLM 8100 spectrofluorimeter at 25 °C. Donor−acceptor labeled and donor-only labeled ribozymes (1 μM) were titrated with $MgCl_2$. The donor (Cy3) fluorescence was excited at 514 nm (2 nm bandwidth) and monitored at 565 nm (8 nm bandwidth). The energy transfer efficiency E as a function of $[Mg^{2+}]$ for each ribozyme construct was calculated using the data from donor only- and donor−acceptor-labeled ribozyme titrations according to eq 1,

$$E = 1 - \frac{F_{DA}}{F_D} \quad (1)$$

where F_{DA} is the donor (Cy3) fluorescence at 565 nm in the presence of acceptor, and F_D is the donor fluorescence at 565 nm in the absence of acceptor. Because of the large spectral separation of donor and acceptor fluorescence emission (565 and 666 nm, respectively), the fluorescence intensity at 565 nm does not contain any significant contribution from the acceptor and can be used without corrections.

For the 4WJ ribozymes and the wild-type 2WJ ribozyme, the data obtained could be described by a simple cooperative binding model:

$$E = E_0 + \Delta E \frac{[Mg^{2+}]^n}{[Mg^{2+}]^n + (K_{d,Mg^{2+}})^n} \quad (2)$$

where E is the energy transfer efficiency at the respective Mg^{2+} concentration, E_0 is the transfer efficiency in the absence of Mg^{2+}, and ΔE is the overall change in FRET efficiency. $K_{d,Mg^{2+}}$ is the equilibrium dissociation constant of the Mg^{2+}−ribozyme complex, and n is a cooperativity parameter.

In kinetic experiments, the time-dependence of donor fluorescence was monitored after addition of 12 mM $MgCl_2$ to a 200 nM solution of donor−acceptor labeled ribozyme (final concentrations of donor strand, other strands are in 2-fold molar excess).

Time-resolved donor emission profiles were collected using time-correlated single photon counting as described (*21*). Pulsed excitation was achieved with a mode-locked argon ion laser at 514 nm and the emission was detected at 530 nm (16 nm band-pass plus 530 nm cutoff filter) under magic angle conditions. The decays were collected in 4096 channels with a time increment of 3 ps/channel.

trFRET Data Analysis. For each ribozyme construct, two separate donor decays were recorded and analyzed. The first, obtained with a sample labeled only with the Cy3 donor, was fitted using a sum of exponential decays (eq 3) to yield the intrinsic donor lifetimes (τ_i) and corresponding decay amplitudes (α_i),

$$I_D(t) = \sum_i \alpha_i \exp\left(-\frac{t}{\tau_i}\right) \quad (3)$$

The decay of the doubly labeled ribozyme−substrate complex was analyzed in terms of two distinct donor−acceptor distance distributions, corresponding to docked and extended conformers (eq 4)

$$I_{DA}(t) = \sum_k f_k \frac{1}{\beta_2 - \beta_1} \int_{\beta_1}^{\beta_2} \int P_k(R) \sum_i \alpha_i \exp\left(-\frac{t}{\tau_i}\left(1 + \frac{\beta R_0^6}{R^6}\right)\right) dR d\beta \quad (4)$$

where k refers to the number of donor−acceptor species, and f_k is the fractional population of each species. For each donor−acceptor species, the corresponding distance is described by the probability distribution $P_k(R)$, which is modeled as a weighted Gaussian function (eq 5)

$$P_k(R) = 4\pi R^2 c_k \exp(-a_k(R - b_k)^2) \quad (5)$$

Each distribution is described by the shape parameters a_k and b_k and the normalizing constant c_k. In eq 4, R_0 is the critical transfer distance at which energy transfer occurs with 50% efficiency, which in the case of the Cy3−Cy5 donor−acceptor pair is 47 Å under the assumption of free rotation of both dyes. However, steady-state anisotropies of 0.31 for Cy3 and Cy5 attached to the ribozyme indicated a restricted movement, necessitating the multiplication of R_0^6 in eq 4 by the correction factor β (*22*). To determine the limiting values for β, the time-resolved anisotropy decay for Cy3 attached to the ribozyme was measured. Because of the limited spectral response of the photomultiplier tube, the anisotropy decay for Cy5 was not accessible experimentally. However, the similar steady-state anisotropies of Cy3 and Cy5 attached to the ribozyme suggested that the time-resolved parameters will also be similar. From the fractional depolarization of the donor due to local rotation, and assuming the same value applies to the acceptor, the range of β values was determined according to Haas et al. (*23*). For Cy3 and Cy5, this analysis indicated that β can adopt values between 0.3 and 3.0, corresponding to β_1 and β_2 in eq 4. The donor decay in eq 4 is averaged over all possible β values, from β_1 to β_2. Donor decays were fitted by adjusting the fractional populations and shape parameters of each distribution for best fit, as judged by the reduced χ^2 value and appearance of weighted residuals. In samples with less than 5% docked conformer, the donor decay was adequately fitted using a single distance term in eq 4.

The equilibrium constant for docking, K_{dock}, is defined as

$$K_{dock} = \frac{\text{fraction docked}}{\text{fraction extended}} \quad (6)$$

which is related to ΔG_{dock} by eq 7:

$$\Delta G_{dock} = -RT \ln K_{dock} \quad (7)$$

with the absolute temperature T, and the general gas constant R, 8.3143 J mol^{-1} K^{-1}.

The destabilization, $\Delta\Delta G_{dock}$, due to a deoxy modification was calculated as the difference between ΔG_{dock} for wild-type and modified ribozymes according to eq 8:

$$\Delta\Delta G_{dock} = \Delta G_{dock}(\text{modified}) - \Delta G_{dock}(\text{wild-type}) \quad (8)$$

leading to positive values for destabilization and negative values for stabilization.

Native Gel Electrophoresis. The structural integrity of 2WJ and 4WJ hairpin ribozymes was verified by native gel electrophoresis in 15% polyacrylamide gels at 25 °C in a thermostated electrophoresis unit. The running buffer was 40 mM Tris/acetate, pH 7.8, 12 mM $MgCl_2$. Ribozyme samples were prepared as for trFRET measurements and mixed with glycerol (50%), and gels were run at a constant current of 35 mA/gel.

Cleavage Activity Tests. For activity tests, the 5′-GCAAGCCACCUCGCAGUCCUA-3′ substrate strand was 5′-phosphorylated with γ-^{32}P-ATP using T4 polynucleotide kinase and gel-purified. Ribozymes were assembled by mixing 1 μM of the donor-labeled strand with 2 μM of all other strands, including traces of the radioactively labeled substrate strand. The annealing procedure was identical to that used in the preparation of the samples for trFRET. Further incubation at 25 °C for 1 h ensured completion of the cleavage reaction. Samples were mixed with loading buffer [8 M urea, 0.025% (w/v) bromphenol blue, 0.025% (w/v) xylene cyanol] and cleaved and noncleaved substrate strands were separated on a 20% acrylamide gel in 8 M urea.

Table 1: Docking Equilibrium Constants, K_{dock}, and Stabilization Energies, ΔG_{dock}, for Modified 2WJ and 4WJ Ribozymes

2WJ	fraction docked	K_{dock}	ΔG_{dock} (kJ mol^{-1})
wt	0.66 ± 0.07	1.9 ± 0.4	−1.6 ± 0.6
dA_{10}	0.50 ± 0.07	0.95 ± 0.24	0.14 ± 0.6
dG_{11}	0.38 ± 0.07	0.62 ± 0.19	1.2 ± 0.8
dA_{24}	0.39 ± 0.04	0.65 ± 0.14	1.1 ± 0.5
dC_{25}	0.27 ± 0.03	0.37 ± 0.07	2.5 ± 0.4
$dA_{10}G_{11}$	<0.05	<0.053	>7.3
$dA_{10}C_{25}$	<0.05	<0.053	>7.3
$dG_{11}A_{24}$	<0.05	<0.053	>7.3
4WJ	**fraction docked**	**K_{dock}**	**ΔG_{dock} (kJ mol^{-1})**
wt	0.84 ± 0.17	5.4 ± 1.7	−4.2 ± 0.8
dA_{10}	0.83 ± 0.14	4.8 ± 1.3	−3.9 ± 0.7
dG_{11}	0.84 ± 0.05	5.2 ± 1.2	−4.1 ± 0.6
dA_{24}	0.80 ± 0.17	3.9 ± 1.2	−3.4 ± 0.8
dC_{25}	0.86 ± 0.02	6.1 ± 1.0	−4.5 ± 0.4
$dA_{10}G_{11}$	0.75 ± 0.11	3.0 ± 0.8	−2.7 ± 0.6
$dA_{10}C_{25}$	0.79 ± 0.32	3.7 ± 2.2	−3.2 ± 1.5
$dG_{11}A_{24}$	0.79 ± 0.11	3.7 ± 0.9	−3.3 ± 0.6

Bands were quantified with a phosphoimaging system (Molecular Dynamics, Storm 820). The overall extent of cleavage was calculated as the ratio of cleaved and non-cleaved substrate strands. Since only 50% of the substrate strands are assembled into a ribozyme and could be cleaved, the fraction of substrate cleaved was multiplied by a factor of 2 in calculating the cleavage efficiency.

RESULTS

To probe the contributions of 2′-hydroxyls to the stability of the docked hairpin ribozyme, we used hairpin ribozymes with a single deoxy modification in position A_{10}, G_{11}, A_{24}, or C_{25}, and with double modifications $A_{10}C_{25}$, $G_{11}A_{24}$, and $A_{10}G_{11}$. All ribozymes contained a Cy3 (donor) and Cy5 (acceptor) label on the 5′-ends of the two helical arms carrying the loops (Figure 1B). The equilibrium distribution of docked and extended conformers was determined by trFRET analysis (Table 1). The various deoxy modifications were examined in the context of both 2WJ and 4WJ forms of the hairpin ribozyme.

With the exception of 2WJ ribozymes with tandem deoxy modifications, the best fits to the donor decays were obtained with two distance distributions centered around mean distances of 26−34 Å and 62−72 Å, corresponding to docked and extended conformers identified previously (*19*). A typical donor decay and distance distribution fit are shown in Figure 2 for the wild-type 2WJ ribozyme. The average distances were constant in all ribozyme constructs within the experimental error (typically ± 5 Å for the docked conformer and ± 10 Å for the extended conformer), indicating that the 2′-deoxy modifications did not perturb the global structures of the docked and extended conformers, with the exception of the 2WJ dG_{11} modification, where the increased donor acceptor distance in the docked conformer (47 Å) indicates some structural rearrangement. The distances recovered from the analysis depend somewhat on the values of β_1 and β_2 in eq 4, but these values were the same in all ribozymes. From the fractional populations of docked and extended conformers, the equilibrium constant for docking, K_{dock}, as well as the free energy of docking, ΔG_{dock}, and the difference in free energy relative to wild-type, $\Delta\Delta G_{dock}$, were calculated as described in Materials and Methods (eqs 6−8).

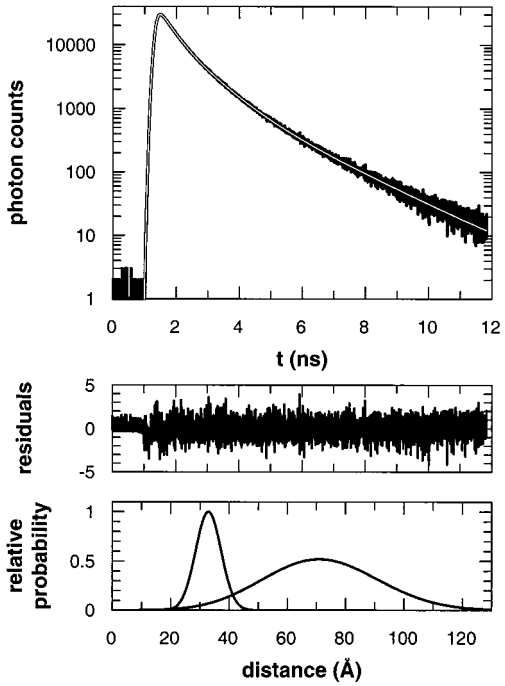

FIGURE 2: Donor fluorescence decay in the presence of acceptor fluorophore (2WJ). The time-resolved fluorescence decay of the donor of a Cy3−Cy5 labeled was analyzed in terms of two distance distributions, reflecting the extended and docked conformers of the ribozyme−substrate complex. The measured donor fluorescence decay (black, upper panel) and the fit (white line) are shown, together with the residuals and the retrieved distance distributions (bottom panel). The distance distribution centered on 35 Å corresponds to the docked conformer, the one centered on 70 Å corresponds to the extended conformer. The distributions are scaled such that the relative heights represent the fractional populations of the two conformers in equilibrium, the ratio of which defines the equilibrium constant. This fit converged to a reduced χ^2 value of 1.1.

Domain docking in the 2WJ ribozyme was strongly destabilized by 2′-deoxy modifications (Table 1 and Figure 3A). Single deoxy modifications lead to a destabilization of the docked conformer between 1.8 kJ mol^{-1} (dA_{10}) and 4.1 kJ mol^{-1} (dC_{25}). In all cases, tandem deoxy modifications reduce the fraction of docked 2WJ complexes to an undetectable level (<5%), corresponding to $\Delta\Delta G_{dock}$ values in excess of 8.9 kJ mol^{-1}. These data suggest that each of the 2′-hydroxyls studied contributes significantly to the tertiary structure stability of the 2WJ ribozyme. As a control, we performed the same experiment with a 2WJ ribozyme carrying a deoxy modification at A_9, which is not involved in hydrogen bonding. This modification causes a destabilization of 1 kJ mol^{-1} (data not shown) and should reflect an upper limit for nonspecific effects of deoxy modifications other than removal of a hydrogen bond.

Surprisingly, no significant destabilization of the docked conformer was detected with the deoxy-modified 4WJ ribozymes under the same conditions (Table 1 and Figure 3B). The greatest destabilization, although still modest, occurs in the $dA_{10}G_{11}$ variant ($\Delta\Delta G_{dock}$ = 1 kJ mol^{-1}). In contrast to this marginal destabilization, the removal of both teeth of the ribose zipper (four hydrogen bonds) destabilizes the *Tetrahymena* ribozyme by 8 kJ mol^{-1} (*24*). The dA_9 control did not show any destabilizing effect on the docked 4WJ ribozyme (data not shown), indicating that the nonspe-

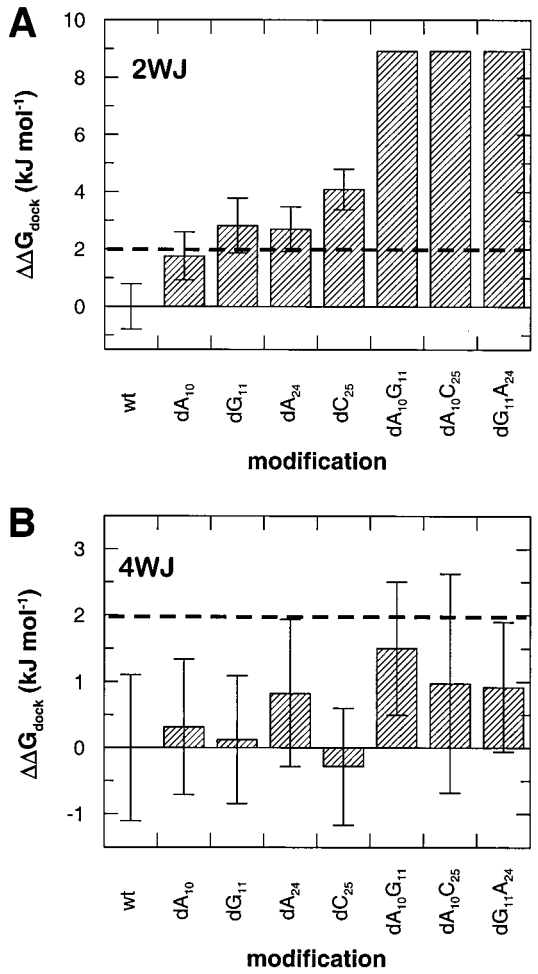

FIGURE 3: Destabilization energies of 2′-deoxy-modified ribozymes in the presence of 12 mM Mg^{2+} as determined from trFRET experiments. From donor−acceptor distance fits, the equilibrium constants of docking were determined as the ratio of the fractional populations of the docked and extended conformers, and the free energy difference between the conformers was calculated. $\Delta\Delta G_{dock}$ values (destabilization in comparison to wild-type) are plotted (A) 2WJ, (B) 4WJ. Note the different energy scales in panels A and B: The destabilizing effect of 2′-deoxy modifications is up to 20 times larger in the 2WJ. The broken line indicates the energetic contribution of a single hydrogen bond in the *Tetrahymena* ribose zipper (*24*).

cific effect of deoxy modifications is also smaller in the 4WJ than in the 2WJ ribozyme.

To verify that the marginal effects observed in the 4WJ were not caused by misfolding of the ribozyme, native gel electrophoresis as well as cleavage activity tests were performed. All ribozyme variants migrated as a single band with the same electrophoretic mobility on native gels in the presence of 12 mM Mg^{2+}, suggesting that the deoxy modifications do not disrupt proper folding. Similarly, all ribozyme variants showed equivalent extent of cleavage (40−50%) with a shortened substrate that forms only three base pairs with the helix adjacent to loop A and therefore dissociates after cleavage and avoids religation. Our results thus suggest that the 2′-hydroxyls studied here do not contribute significantly to the thermodynamic stability of the docked 4WJ ribozyme conformer.

Since tertiary structure formation in the hairpin ribozyme is linked to Mg^{2+} ion binding (*8*, *19*), as in many other RNA molecules, we also examined the Mg^{2+} binding properties of the deoxy-modified ribozymes. Mg^{2+} ion binding isotherms (Figure 4) were obtained by measuring the steady-state FRET efficiency as a function of [Mg^{2+}].

In the context of a 2WJ, the Mg^{2+} binding isotherms are altered significantly in both amplitude and shape (Figure 4A). While the wild-type 2WJ ribozyme binds Mg^{2+} with a K_d of 1.6 mM and a cooperativity coefficient of 0.84, the titration data for the deoxy-modified 2WJ ribozymes cannot be described by the simple cooperative binding model (eq 2) but instead exhibit two transitions. Moreover, the titration profiles are reduced in amplitude as compared to the wild-type ribozyme and do not reach saturation, even at the highest [Mg^{2+}] used (230 mM). Thus, the Mg^{2+} binding properties of the 2WJ ribozymes are significantly perturbed by any of the 2′-deoxy modifications.

In contrast, the Mg^{2+} binding isotherms for the modified 4WJ ribozymes resemble the one for the wild-type over a wide range of [Mg^{2+}] (Figure 4B), indicating that Mg^{2+} binding is not significantly perturbed. The K_d values for Mg^{2+} range from 0.29 mM (wild-type) to 0.91 mM ($dA_{10}G_{11}$). The amplitudes of the binding isotherms are similar for all 4WJ constructs, and the cooperativity coefficient (see eq 2) is between 0.9 and 1.3. Thus, the 2′-deoxy modifications do not significantly alter Mg^{2+} binding in the context of a 4WJ ribozyme. This is consistent with the absence of any significant destabilization of the docked tertiary structure of the deoxy-modified 4WJ ribozymes. In a previous steady-state FRET study of dA_{10} and dC_{25} modified ribozymes, slightly larger effects of the deoxy modifications were found (*18*).

The steady-state FRET data (Figure 4A,B) are also in accord with the results of the trFRET analysis. At 12 mM Mg^{2+}, the steady-state FRET efficiency is similar for all the 4WJ ribozymes, confirming that the net energetic contribution of the 2′-hydroxyls to docking is marginal. For the 2WJ ribozymes, the order of relative FRET efficiencies is consistent with the docking propensity as determined from trFRET.

In view of the significant differences in tertiary structure stabilization in 2WJ ribozyme variants, it was interesting to examine whether their docking kinetics are also different. Kinetic transients were measured as a decrease in donor fluorescence after addition of 12 mM Mg^{2+} to induce docking (data not shown). The 2′-deoxy modifications in the 2WJ ribozyme have a significant effect on the amplitude of the kinetic profiles, while for the 4WJ, consistent with the marginal effect of the 2′-deoxy modifications on the tertiary structure stability, the kinetic traces for domain docking of the modified ribozymes are similar in rate and amplitude. Again, the docking amplitudes in the kinetic experiments agree reasonably well with the degree of docking from steady-state FRET and trFRET data at 12 mM Mg^{2+}. All observed traces show at least two kinetic phases, preventing a straightforward mechanistic interpretation of the docking kinetics.

DISCUSSION

trFRET Analysis Quantifies the Energetic Importance of Ground-State Interactions. Almost all studies to identify tertiary interactions in the hairpin ribozyme have used a minimal 2WJ ribozyme and catalytic activity as a probe.

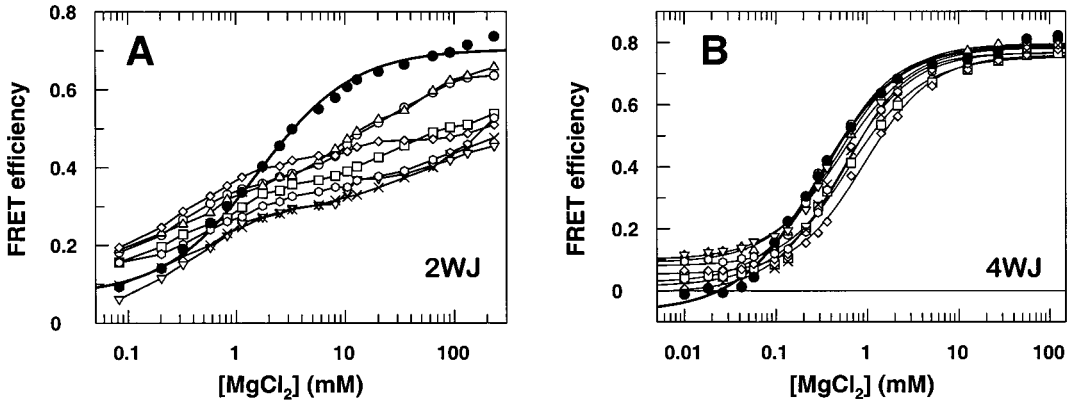

FIGURE 4: Effect of the 2′-deoxy modifications on Mg^{2+} binding. Mg^{2+} titrations. (A) 2WJ, (B) 4WJ. Wild-type ribozymes are plotted with filled symbols (●), variants with open symbols (○ dA_{10}, □ dG_{11}, Δ dA_{24}, ▽ dC_{25}, ◊ $dA_{10}G_{11}$, ⬡ $A_{10}C_{25}$, × $dG_{11}A_{24}$). Mg^{2+} binding was monitored as an increase in fluorescence resonance energy transfer from Cy3 to Cy5 upon docking in steady-state titrations. While the 2′-deoxy modifications do not affect Mg^{2+} binding in context of a 4WJ to a significant extent, all of them perturb Mg^{2+} binding in the 2WJ ribozyme. Both shape and amplitude of the Mg^{2+} binding isotherms are affected.

Notably, 2′-deoxy modifications of A_{10}, G_{11}, A_{24}, or C_{25} each abolish the catalytic activity (*11*), indicating that the 2′-hydroxyls are required for docking or are directly involved in catalysis. In general, functional groups identified on the basis of mutational or chemical modification studies using catalytic activity as a probe might be involved in tertiary interactions in the ground-state of the ribozyme−substrate complex or in the stabilization of the transition state. FRET analysis of modified hairpin ribozymes is a suitable technique for assessing ground-state interactions. Steady-state FRET experiments have shown that deoxy modifications of A_{10} and C_{25} interfere with the tertiary folding of the hairpin ribozyme in its natural 4WJ form (*18*), while kinetic FRET experiments have shown that 2′-deoxy substitutions at A_{10} and G_{11} inhibit docking in a minimal 2WJ ribozyme (*6*). In neither of these studies were the effects of deoxy modifications quantified in terms of the energetic destabilization of the docked ribozyme−substrate complex. In contrast, the trFRET analysis presented here provides a quantitative method to assess the energetic importance of ground-state interactions. Equilibrium populations of docked and extended conformers can be determined to define the equilibrium constant and free energy of docking, K_{dock} and ΔG_{dock}, respectively. Ground-state interactions are identified from modifications that alter the docking equilibrium, and the difference in stabilization energy of the modified ribozyme as compared to the wild-type ribozyme, $\Delta\Delta G_{dock}$, can be calculated. Thus, the present trFRET data on the deoxy-modified ribozymes provide a direct measurement of the contributions of each 2′-hydroxyl group to the thermodynamic stability of the docked conformer in the ground state.

The 2′-Hydroxyls of A_{10}, G_{11}, A_{24}, and C_{25} Stabilize the Docked 2WJ Hairpin Ribozyme. In the 2WJ ribozyme, single 2′-deoxy modifications destabilize the docked conformer by 1.8 kJ mol^{-1} (dA_{10}) to 4.1 kJ mol^{-1} (dC_{25}). The degree of destabilization is in agreement with the hydrogen bonding pattern seen in the crystal structure (Figure 1A, *10*), which predicts larger effects for dG_{11} and dC_{25} (two hydrogen bonds removed in each case) than for dA_{10} and dA_{24} (one hydrogen bond removed). In comparison with the stabilization by 2 kJ mol^{-1} from one hydrogen bond determined for the *Tetrahymena* ribose zipper (*24*), the 2′-hydroxyl of C_{25} appears to contribute a stabilization energy equivalent to two hydrogen bonds, while the 2′-hydroxyl of A_{10} contributes one equivalent. The stabilization provided by the 2′-hydroxyls of G_{11} and A_{24}, however, is between one and two equivalents. In these cases, additional effects might influence the $\Delta\Delta G_{dock}$ values. First, the fate of the remaining unsatisfied hydrogen bonding partner can contribute to the energy difference observed experimentally (*25*, *26*). Second, 2′-deoxy modifications not only remove a hydrogen bond donor and acceptor (specific effect), but additionally change the sugar pucker from 3′-endo to 2′-endo and create a cavity (nonspecific effect). Such effects may obscure a simple pattern of expected destabilization energies. For single deoxy modifications in the 2WJ ribozyme, the nonspecific effects provide a small contribution to the $\Delta\Delta G_{dock}$ values, as can be deduced from a deoxy modification at A_9 that destabilizes the docked 2WJ ribozyme by ca. 1 kJ mol^{-1}. A_9 is within 6 Å of the catalytic core of the hairpin ribozyme (*10*) and presumably rather sensitive to subtle changes. Therefore, we expect the effect measured to represent an upper limit for nonspecific effects due to deoxy modifications. Thus, the main contribution to the $\Delta\Delta G_{dock}$ values measured results from the removal of a hydrogen bond.

With tandem deoxy modifications, secondary effects appear to be more deleterious and could account for the strong destabilization observed that are inconsistent with the hydrogen bonding pattern (Figure 1A). For example, removal of the 2′-hydroxyl of G_{11} should not have an additional destabilizing effect in a dA_{24} background, provided that the 2′-hydroxyls at G_{11} and A_{24} interact with each other as seen in the crystal structure. However, the destabilization observed for $dG_{11}A_{24}$ is higher than the additive effect of the single dG_{11} and dA_{24} modifications. It has been shown that in single-stranded regions, deoxy modifications can alter the RNA backbone up to a distance of three nucleotides from the modification (*27*). These backbone alterations depend on the position of the nucleotide and would therefore provide different contributions in the different constructs and will be more severe in double modifications. The excess in destabilization due to $dG_{11}A_{24}$ could be due to these effects. The same is true for $dA_{10}C_{25}$ and, to a smaller extent, for $dA_{10}G_{11}$. Thus, the results with the doubly modified ribozymes cannot be interpreted in terms of isolated energetic contributions from hydrogen bonds alone.

No Energetic Contribution from Ribose Zipper Hydrogen Bonds in the Ground-State of the Natural 4WJ Hairpin Ribozyme. Interestingly, the same 2′-deoxy modifications that lead to a significant destabilization of the docked conformer in the context of the 2WJ ribozyme have only a marginal effect on the stability of the docked 4WJ ribozyme. Single 2′-deoxy modifications lead to a destabilization of less than 1 kJ mol^{-1}. The energetic contributions of each of the four hydroxyl groups are significantly smaller than the 2 kJ mol^{-1} per hydrogen bond determined for the *Tetrahymena* ribozyme ribose zipper (*24*). Although the 4WJ ribozyme is intrinsically more stable than its 2WJ counterpart, a destabilization by 2 kJ mol^{-1} should have been readily resolved in the trFRET (and steady-state FRET) measurements. It is likely that the modest destabilization energies in the 4WJ reflect nonspecific effects, as outlined above for the 2WJ, and the slight differences in Mg^{2+} binding. Interestingly, the dA_9 control did not show a significant destabilizing effect, corroborating the notion that the nonspecific effects due to a deoxy modification are minor in the 4WJ ribozyme.

Slight adjustments in local structure can allow formation of alternate hydrogen bonds (with a different group of the RNA or water) that compensate for the one removed, leading to only a small net effect. It seems unlikely, however, that such rearrangements occur in the rather rigid 4WJ ribozyme, while the more flexible 2WJ ribozyme (*20*) apparently cannot accommodate these alterations with the same efficiency. The modest destabilization due to the 2′-deoxy modifications, therefore, suggests that the ribose zipper hydrogen bonds do not contribute significantly to the thermodynamic stability of the docked 4WJ ribozyme.

While proper folding of the ribozymes was verified in native gel electrophoresis, the small effects observed with the modified 4WJ ribozymes could indicate that the variants studied have formed a pseudo-docked conformation with a donor−acceptor distance similar to the true docked conformer but have not formed specific tertiary loop−loop interactions required for catalytic activity. Indeed, a 4WJ with base-paired regions instead of the loops forms a conformer with similar geometry to the docked ribozyme (*19*, *28*). This variant is not catalytically active and requires millimolar concentrations of Mg^{2+} for folding (*28*). At 12 mM Mg^{2+}, as used here, the pseudo-docked conformer is populated to about 35%, as revealed in a previous trFRET study (*19*). Several lines of evidence suggest that this pseudo-docked conformer is not responsible for our findings. First, cleavage activity tests showed that all 4WJ ribozymes are 40−50% active. While 85% of the wild-type ribozyme are docked in equilibrium, according to the present trFRET measurements, ∼35% are in the pseudo-docked conformation (*19*), and thus about 50% of the ribozyme can contribute to catalytic activity, which is in good agreement with the activity assay. Second, the Mg^{2+} titrations yield K_d values between 0.29 and 0.91 mM, indicating that less Mg^{2+} is required for docking of the 4WJ ribozymes than for the pseudo-docked conformer (3 mM, 28). This further confirms that the species with short donor−acceptor distance is the specifically docked conformer [at least the excess over 35%]. We cannot exclude the possibility that the bulky Cy3 and Cy5 fluorophores exert some inhibitory effect on docking, which would explain the somewhat smaller fraction of docked conformers as compared to a previous trFRET study using longer dye linkers (*19*). However, it is reasonable to assume that this effect, if present, as well as the fraction of the pseudo-docked conformer, will be constant for the deoxy-variants and therefore does not affect the comparison of $\Delta\Delta G_{dock}$ values (Figure 3).

Tertiary Structure Stabilization in the 2WJ and 4WJ Ribozymes is Different. The trFRET results for the 2′-deoxy-modified ribozymes indicate that the four 2′-hydroxyl groups examined contribute to the stability of the docked complex in the context of the 2WJ but not the 4WJ, pointing to different energetic contributions in the two forms of the ribozyme. In addition, the metal ion titrations reveal altered Mg^{2+} binding properties of the 2′-deoxy variants in the 2WJ ribozyme but not in the 4WJ ribozyme. In the 2WJ, the observation that the deoxy modifications disrupt Mg^{2+} binding does not necessarily imply that the 2′-hydroxyl groups coordinate Mg^{2+} directly. Rather, the binding of metal ions to the ribozyme is thermodynamically coupled to tertiary structure formation. Because of this coupling, any destabilization of the tertiary structure will be reflected in weakened binding of Mg^{2+} to the hairpin ribozyme. In the 4WJ, Mg^{2+} binding is not affected by any of the deoxy modifications, which is again consistent with the marginal destabilization of the tertiary structure.

The different effects of the 2′-hydroxyl modifications in the context of a 2WJ and 4WJ suggest that either the tertiary structure is different in the two ribozyme forms, or the underlying energetics are different. A significant body of evidence argues against the structures being different, however. First, the hairpin ribozyme is active both in the context of a 2WJ and a 4WJ, suggesting that at least the transition state is similar in each case. Second, trFRET measurements reveal the same distances between the ends of the helical arms carrying loops A and B in the docked 2WJ and 4WJ ribozymes (*19*, *20*), indicating the interarm angles are the similar. Third, the ribose zipper motif that had been probed in the minimal 2WJ ribozyme (*4*, *11*−*13*), is present in the crystal structure of the 4WJ ribozyme (*10*). As the most important evidence, the structure of the natural 4WJ is consistent with a body of biochemical data derived from studies of the 2WJ ribozyme (*10*).

A different contribution of a specific interaction to the tertiary structure stability of the minimal and natural hairpin ribozymes, on the other hand, is very well possible. Changing G_{+1} in the substrate strand to A reduces docking of the 4WJ ribozyme by a factor of 2 as compared to wild-type but completely abolishes docking of a 2WJ ribozyme (*19*). Furthermore, the docking thermodynamics for the 2WJ and 4WJ ribozymes differ with respect to enthalpic and entropic contributions. A larger contribution from ribose zipper hydrogen bonds in the 2WJ might explain our previous observation of a more favorable enthalpic contribution for 2WJ docking than for the 4WJ (*20*) and support the notion that the flexible 2WJ allows for optimum alignment of hydrogen bonds that are not as important for the tertiary structure stability of the inherently more rigid 4WJ. Our trFRET measurements on dA_9 ribozymes demonstrate that, similarly, nonspecific effects give rise to different effects in the 2WJ and 4WJ constructs.

Notably, in the 4WJ ribozyme, the secondary and tertiary structure transitions are thermodynamically coupled, while they are separated in the 2WJ ribozyme (*20*), which points

to a different balance between the secondary and tertiary structures. NMR studies on the folding of the *Tetrahymena* ribozyme have shown that the P5abc three-helix junction in the P4−P6 domain undergoes secondary structure rearrangements upon tertiary structure formation (*29*). The balance between secondary and tertiary structure formation can be shifted by mutations, which exhibit different effects in the isolated P5abc junction than in the complete P4−P6 domain (*30*). This illustrates that tertiary interactions in RNAs are context-dependent and imply that findings on isolated domains do not necessarily reflect the situation in the background of a larger RNA molecule. Similarly, the minimal 2WJ ribozyme provides a qualitatively different background than the natural 4WJ ribozyme, which appears to result in different energetics of tertiary interactions.

Hydrogen Bonds in RNA Teriary Structure. Our results suggest that hydrogen bonds involving 2′-hydroxyls do not confer a significant amount of thermodynamic stability to RNA tertiary structure in the natural hairpin ribozyme. A moderate energetic contribution of hydrogen bonds seems to be a more general feature of RNA tertiary structures: Even though the contribution of the ribose zipper in the *Tetrahymena* ribozyme (*24*) is larger than the effects seen with the hairpin ribozyme, a value of 2 kJ mol^{-1} for a hydrogen bond is smaller than the stability derived from hydrogen bonds in proteins [2.1−16.7 kJ mol^{-1} (*25*, *31*−*33*)]. A contribution of 2−4 kJ mol^{-1} has been measured for hydrogen bonds involved in RNA secondary structure stabilization (*34*). The upper limit for the energetic contribution of hydrogen bonds in base pairs was estimated to be 8 kJ mol^{-1} (*35*). It is conceivable that the contributions of hydrogen bonds between complementary bases and tertiary hydrogen bonds differ due to the different polarity (dielectric constant) of the local environment: In contrast to the rather nonpolar context of base-pair formation, tertiary hydrogen bonds are formed within the context of a highly charged backbone, which reduces electrostatic contributions. Studies on a RNA hairpin revealed that the hydrogen bond free energy is highly context-dependent, with a contribution of about 4 kJ mol^{-1} for bases in the stem region and less than 2.8 kJ mol^{-1} in the loop region (*36*).

Altogether, our results suggest that the 2WJ ribozyme is not an appropriate model system to study the energetics of tertiary interactions in the active hairpin ribozyme. Using minimal systems, caution is necessary in quantitative interpretation of thermodynamic data due to the context dependence of tertiary interactions in RNA.

ACKNOWLEDGMENT

We thank Martha Fedor for stimulating discussions and helpful suggestions, Adrian Ferre-d'Amare for sharing coordinates prior to publication, Jeffrey Orr for help in implementing new functions in the distance fitting program and sharing his experience in RNA purification, Lori Lebruska and Tracy Vivlemore for help with cleavage activity tests, and Markus Rudolph for helpful comments on the manuscript.

REFERENCES

1. Fedor, M. J. (1999) *J. Mol. Biol. 297*, 269−291.
2. Komatsu, Y., Koizumi, M., Nakamura, H., and Ohtsuka, E. (1994) *J. Am. Chem. Soc. 116*, 3692−3696.
3. Feldstein, P. A., and Bruening, G. (1993) *Nucleic Acids Res. 21*, 1991−1998.
4. Earnshaw, D. J., Masquida, B., Müller, S., Sigurdson, S. T., Eckstein, F., Westhof, E., and Gait, M. J. (1997) *J. Mol. Biol. 274*, 197−212.
5. Pinard, R., Heckman, J. E., and Burke, J. M. (1999) *J. Mol. Biol. 287*, 239−251.
6. Walter, N. G., Hampel, K. J., Brown, K. M., and Burke, J. M. (1998) *EMBO J. 17*, 2378−2391.
7. Murchie, A. I., Thomson, J. B., Walter, F., and Lilley, D. M. (1998) *Mol. Cell 1*, 873−881.
8. Walter, F., Murchie, A. I. H., Thomson, J. B., and Lilley, D. M. J. (1998) *Biochemistry 37*, 14195−14203.
9. Hampel, K. J., Walter, N. G., and Burke, J. M. (1998) *Biochemistry 37*, 14672−14682.
10. Rupert, P. B., and Ferre-D'Amare, A. R. (2001) *Nature 401*, 780−786.
11. Chowrira, B. M., Berzal-Herranz, A., Keller, C. F., and Burke, J. M. (1993) *J. Biol. Chem. 268*, 19548−19562.
12. Ryder, S. P., and Strobel, S. A. (1999) *J. Mol. Biol. 291*, 295−311.
13. Earnshaw, D. J., Hamm, M. L., Piccirilli, J. A., Karpeisky, A, Beigelman, L., Ross, B. S., Manoharan, M., and Gait, M. J. (2000) *Biochemistry 39*, 6410−6421.
14. Cate, J. H., Gooding, A. R., Podell, E., Zhou, K., Golden, B. L., Kundrot, C. E., Cech, T. R., and Doudna, J. A. (1996) *Science 273*, 1678−1685.
15. Ferre-D'Amare, A. R., Zhou, K., and Doudna, J. A. (1998) *Nature 395*, 567−574.
16. Conn, G. L., Draper, D. E., Lattman, E. E., and Gittis, A. G. (1999) *Science 284*, 1171−1174.
17. Wimberly, B. T., Guymon, R., McCutcheon, J. P., White, S. W., and Ramakrishnan, V. (1999) *Cell 97*, 491−502.
18. Wilson, T., Zhao, Z.-Y., Maxwell, K., Kontogiannis, L., and Lilley, D. M. J. (2001) *Biochemistry 40*, 2291−2302.
19. Walter, N. G., Burke, J. M., and Millar, D. P. (1999) *Nat. Struct. Biol. 6*, 544−549.
20. Klostermeier, D., and Millar, D. P. (2000) *Biochemistry, 39*, 12970−12978.
21. Eis, P. S., and Millar, D. P. (1993) *Biochemistry 32*, 13852−13860.
22. Albaugh, S., and Steiner, R. F. (1989) *J. Phys. Chem. 93*, 8013−8016.
23. Haas, E., Katzir, E.-K., and Steinberg, I. Z. (1978) *Biochemistry 17*, 5064−5070.
24. Silverman, S. K., and Cech, T. R. (1999) *Biochemistry 38*, 8691−8702.
25. Shirley, B. A., Stanssens, P., Hahn, U., and Pace, C. N. (1992) *Biochemistry 31*, 725−732.
26. Pace, C. N. (1995) *Methods Enzymol. 259*, 538−554.
27. Lindqvist, M., Sarkar, M., Winqvist, A., Rozners, E., Stromberg, R., and Graslund, A. (2000) *Biochemistry 39*, 1693−1701.
28. Zhao, Z.-Y., Wilson, T., Maxwell, K., and Lilley, D. M. J. (2000) *RNA 6*, 1833−1846.
29. Wu, M., and Tinoco, I. (1998) *Proc. Natl. Acad. Sci. U.S.A. 95*, 11555−11560.
30. Silverman, S. K., Zheng, M., Wu, M., Tinoco, I., and Cech, T. R. (1999) *RNA 5*, 1665−1674.
31. Jeffrey, G. A., and Saenger, W. (1991) in *Hydrogen Bonding in Biological Structures*, Springer, Berlin.
32. Fersht, A. R. (1987) *Trends Biochem. Sci. 12*, 301−304.
33. Byrne, M. P., Manuel, R. L., Lowe, L. G., and Stites, W. E. (1995) *Biochemistry 34*, 13949−13960.
34. Freier, S. M., Sugimoto, N., Sinclair, A., Alkema, D., Neilson, T., Kierzek, R., Caruthers, M. H., and Turner, D. (1986) *Biochemistry 25*, 3214−3219.
35. Turner, D. H., Sugimoto, N., Kierzek, R., and Dreiker S. D. (1987) *J. Am. Chem. Soc. 109*, 3783−3785.
36. SantaLucia, J., Kierzek, R., and Turner, D. (1992) *Science 256*, 217−219.

BI010773F